

(Fig. 3) are referred to as whistler wings. The name describes both the structure and the fact that the perturbations are carried in the whistler mode (14) [analogous structures in which the perturbations are carried along the magnetic field by Alfvén waves while being swept downstream by a flowing plasma were originally described for the MHD limit (15) and were called Alfvén wings]. The perturbation in the whistler mode has to our knowledge been reported only in laboratory experiments. The experiments (16) were carried out in a regime for which the spatial scale of the obstacle was small compared with the ion gyro radii and large compared with the electron gyro radii, which corresponds to the circumstances of our measurements [this unusual regime has also been studied in a spacecraft barium release (17) but never before in a natural context].

Several other instruments (8, 9, 18) on the Galileo spacecraft made in situ measurements that will be useful for improvement of the analysis presented here. Small changes in flow direction linked to the diversion of the flow around the obstacle could possibly be observed by the electron sensors of the Plasma Instrumentation (PLS) (8) and the Energetic Particle Detector (EPD) (18), although the angular changes are probably too small to be reliably identified. Both instruments may be able to search for a local population of heavy ions to check whether we have been premature in ruling out a comet-like interaction.

It will also be of interest to see if the magnetosonic-whistler waves that carry the pressure perturbations can be detected. The power in these waves is expected to peak at ~ 3 Hz in the plasma rest frame, but they will be Doppler-shifted by the flow to much lower frequencies in the spacecraft frame. Further work will be needed to extract evidence of these Doppler-shifted waves from the magnetometer data.

If electrons can be trapped in the magnetospheric cavity surrounding Gaspra, they may radiate electromagnetic power near the electron cyclotron frequency, much as electrons at low altitudes in the Jovian magnetosphere produce ~ 10 -MHz (decametric) emissions (19). The inferred magnetic moment of Gaspra constrains the frequencies of such an emission to the band below 100 kHz for the lower estimated magnetic moment and below 4 MHz for the higher estimate. Enhanced power within this range of frequencies in the spectra of the Plasma Wave System (PWS) (9) would support the interpretation that we have provided, but initial results do not show any signals.

These observations provide a rationale for outfitting asteroid-bound spacecraft with magnetometers. They also suggest further investigation of the relevant parameter re-

gime in laboratory experiments and computer simulations.

REFERENCES AND NOTES

1. M. J. S. Belton *et al.*, *Science* **257**, 1647 (1992).
2. F. P. Fanale, B. E. Clark, J. F. Bell, *J. Geophys. Res.* **97**, 20863 (1992).
3. M. G. Kivelson *et al.*, *Space Sci. Rev.* **60**, 357 (1992).
4. Because of the 10-month gap in high-resolution data after the flyby of Earth in late 1990, it was necessary to determine the offset for the magnetic field sensor aligned with the spacecraft spin axis from the limited data available at Gaspra. If the wrong offset is used, the magnitude of the field appears to change when the field merely rotates. Because the solar wind magnitude typically changes little across discontinuities, we selected an offset that minimized the variations of the field magnitude in a dataset that did not include the 4 min of data around Gaspra. The variability of the field magnitude associated with the large rotations near closest approach was then small.
5. J. Luhmann *et al.*, *J. Geophys. Res.* **91**, 3001 (1986).
6. T. Ogino, R. J. Walker, M. Ashour-Abdalla, *IEEE Trans. Plasma Sci.* **20**, 487 (1992).
7. R. E. Holzer and J. A. Slavin, *J. Geophys. Res.* **83**, 3831 (1978).
8. L. Frank *et al.*, *Space Sci. Rev.* **60**, 283 (1992).
9. D. Gurnett *et al.*, *ibid.*, p. 341.
10. N. Sugiura and D. W. Strangway, in *Meteorites and the Early Solar System*, J. F. Kerridge and M. S. Matthews, Eds. (Univ. of Arizona Press, Tucson, 1988), pp. 595-615.
11. C. P. Sonett, *Geophys. Res. Lett.* **5**, 151 (1978).
12. J. R. Spreiter and A. Y. Alksne, *Annu. Rev. Fluid Mech.* **2**, 313 (1970).
13. See, for example, V. Formisano and C. F. Kennel, *J. Plasma Phys.* **3**, 55 (1969); T. J. M. Boyd and J. J. Sanderson, *Plasma Dynamics* (Barnes and Noble, New York, 1969), p. 191.
14. E. W. Greenstadt, in *Physical Studies of Minor Planets*, T. Gehrels, Ed. (National Aeronautics and Space Administration SP-267, Washington, DC, 1971), pp. 567-575; *Icarus* **14**, 374 (1971).
15. S. D. Drell, H. M. Foley, M. A. Ruderman, *J. Geophys. Res.* **70**, 3131 (1965).
16. R. L. Stenzel and J. M. Urrutia, *Geophys. Res. Lett.* **16**, 361 (1989).
17. H. Luhr *et al.*, *Nature* **320**, 10 (1986).
18. D. J. Williams *et al.*, *Space Sci. Rev.* **60**, 385 (1992).
19. D. A. Gurnett and F. L. Scarf, in *Physics of the Jovian Magnetosphere*, A. J. Dessler, Ed. (Cambridge Univ. Press, New York, 1983), pp. 285-316; T. D. Carr, M. D. Desch, J. K. Alexander, *ibid.*, pp. 226-284.
20. We thank C. Polanskey, T. Johnson, S. Joy, C. F. Kennel, T. King, C. T. Russell, and J. T. Wasson for their essential contributions to this work. We are grateful to the Galileo team at the Jet Propulsion Laboratory (JPL), especially T. Johnson and W. O'Neil. We thank D. Gurnett for providing a preview of the data from his instrument. This work was partially supported by JPL under contract no. 958694.

29 January 1993; accepted 27 May 1993

Experimental Realization of the Covalent Solid Carbon Nitride

Chunming Niu, Yuan Z. Lu, Charles M. Lieber*

Pulsed laser ablation of graphite targets combined with an intense, atomic nitrogen source has been used to prepare C-N thin film materials. The average nitrogen content in the films was systematically varied by controlling atomic nitrogen flux. Rutherford backscattering measurements show that up to 40 percent nitrogen can be incorporated on average into these solids under the present reaction conditions. Photoelectron spectroscopy further indicates that carbon and nitrogen form an unpolarized covalent bond in these C-N materials. Qualitative tests indicate that the C-N solids are thermally robust and hard. In addition, strong electron diffraction is observed from crystallites within the films. Notably, analysis of these diffraction data show that the only viable structure for the C-N crystallites is that of β -C₃N₄, a material predicted theoretically to exhibit superhardness. The experimental synthesis of this new C-N material offers exciting prospects for both basic research and engineering applications.

The development of new materials exhibiting useful mechanical, electronic, or magnetic properties represents a central challenge of materials research (1). Among the wide array of important properties, hardness is a material characteristic that may be possible to understand with current theory,

and thus it represents an ideal one in which to test our ability to design materials with predictable properties. Because hardness is also one material property that is essential to many high-performance engineering applications, this endeavor is of great technological importance as well (2). Hardness can be well represented by the bulk modulus of an ideal solid. Both empirical and ab initio calculations have shown that a large bulk modulus (and corresponding hardness) require short, covalent bonds within a solid (3, 4). Notably, it was predicted on the basis of these theoretical ideas that the covalent carbon-nitrogen solid, β -C₃N₄,

C. Niu, Department of Chemistry, Harvard University, Cambridge, MA 02138.

Y. Z. Lu, Materials Research Laboratory, Harvard University, Cambridge, MA 02138.

C. M. Lieber, Department of Chemistry and Division of Applied Sciences, Harvard University, Cambridge, MA 02138.

*To whom correspondence should be addressed.

would have a bulk modulus comparable to or greater than the hardest known material, diamond (4). In this work it was assumed that $\beta\text{-C}_3\text{N}_4$ would adopt the known structure of Si_3N_4 (5), thus consisting of a network of CN_4 tetrahedra linked at the corners by threefold coordinate N atoms (Fig. 1). Interestingly, these calculations further showed that the cohesive energy of $\beta\text{-C}_3\text{N}_4$ should be sufficiently large to yield a metastable solid. Experimental efforts to date, however, have failed to yield this hypothesized, superhard material.

Herein, we report the synthesis of carbon-nitrogen (C-N) materials and structural evidence for the formation of $\beta\text{-C}_3\text{N}_4$. Pulsed laser ablation of graphite targets combined with a high-flux, atomic nitrogen source has been used to prepare C-N thin films in which the nitrogen content was controlled systematically by means of this unique nitrogen source. Compositional and spectroscopic analyses show that the films contain only C and N, and that the bonding in the solids is covalent. Qualitative tests also indicate that these C-N films are thermally robust and hard. In addition, strong electron diffraction is observed from crystallites within the films, and notably, these diffraction data indicate that the only viable structure for the C-N crystallites is that of $\beta\text{-C}_3\text{N}_4$. Our studies thus provide strong support for the theoretical approach used to predict the stability of this solid, but more importantly, these data demonstrate the synthesis of a new material with potentially wide-ranging applications.

Several approaches have been used previously in attempts to prepare $\beta\text{-C}_3\text{N}_4$ (6–9). Plasma decomposition of CH_4 and N_2 (6) and pyrolytic decomposition of C-N-H organics (7) led to the formation of amorphous C-N-H solids and no evidence for $\beta\text{-C}_3\text{N}_4$. It is likely that the stability of C-H and N-H products under the reaction conditions used in these studies preclude the formation of $\beta\text{-C}_3\text{N}_4$. Shockwave compression of organic C-N-H precursors was also used in attempts to prepare $\beta\text{-C}_3\text{N}_4$ (8). The $\beta\text{-C}_3\text{N}_4$ target was not detected among the products detected in this work, although well-ordered diamond was observed. It is possible that the poor control of reaction energetics, in the starting materials, or both contributed to the failure of these latter investigations.

To overcome potential thermodynamic and kinetic limitations to the formation of $\beta\text{-C}_3\text{N}_4$ we have devised a synthetic approach that involves the combination of energetic carbon species with atomic nitrogen, and subsequent trapping of the resulting C-N products during low-temperature thin film growth (Fig. 2). A pulsed Nd:YAG laser (10) was used to ablate a high-purity graphite target within a stain-

less steel vacuum chamber. The ablation plume, which contains a variety of carbon fragments (11), was directed at a diametrically opposed substrate [Si(100) or polycrystalline Ni] located 4 cm from the target. A unique feature of our synthetic apparatus is the atomic beam source used to incorporate reactive atomic species into the ablation products. Herein, atomic nitrogen is controllably incorporated into the carbon fragments by means of a continuous flow, high-flux source that intersects the ablation plume at the substrate surface (Fig. 2). This atomic nitrogen beam is created by a radio frequency (RF) discharge within an Al_2O_3 nozzle through which a relatively high pressure (≈ 100 torr) N_2 -seeded He flow passes. This source can produce a very high flux of atomic nitrogen ($> 10^{18}$ atom sr^{-1} s^{-1}) with kinetic energies exceeding 1 eV (12). In addition, the flux can be systematically changed through variations in the N_2 to He ratio.

This apparatus was used to prepare a series of carbon nitrogen thin films where the relative flux of atomic nitrogen and substrate temperature have been systematically varied during growth. In all cases the chemical composition of the films was determined with Rutherford backscattering spectroscopy (RBS). Representative RBS data obtained on a series of C-N films grown on Si(100) substrates with a 150-W RF discharge and 1, 4, and 12% N_2 in He are shown in Fig. 3. It is immediately

evident upon examination of the RBS data that the fraction of nitrogen in the C-N films increases systematically as the percentage N_2 in beam source is increased from 1 to 12%. Quantitative analysis of the RBS data shows that the use of beams with 1, 4, and 12% N_2 yields C-N films with average nitrogen contents of 15, 28, and 41%, respectively. Although the largest average percentage nitrogen obtained reproducibly in these films (45%) is less than that expected for the ideal $\beta\text{-C}_3\text{N}_4$ solid (57%), the concentration of nitrogen in local regions of the films may be both higher and lower than the average values determined by RBS. Hence, some regions of the C-N solid could very well have the correct C_3N_4 stoichiometry. Nevertheless, it is important to note that our thin films contain the highest fractions of nitrogen yet observed in pure binary C-N solids.

In addition, several experiments have also been carried out to determine the influence of the source of nitrogen and substrate growth temperature. Importantly, essentially no nitrogen (<1%) is incorporated into films prepared by laser ablation of graphite with the RF discharge off or in a background of 200 mtorr of N_2 ; that is, these films consist only of amorphous carbon. Hence, the generation and reaction of atomic nitrogen with the carbon fragments produced by laser ablation is essential to the formation of the C-N films. Secondly, film

Fig. 1. Computer model of $\beta\text{-C}_3\text{N}_4$ displaying a single unit cell. The structure is based on the known structure of $\beta\text{-Si}_3\text{N}_4$ and theoretically calculated bond lengths (4). Each sp^3 -hybridized carbon atom (black) is bonded to four nitrogen atoms (gray) in a distorted tetrahedral geometry. Each sp^2 -hybridized nitrogen atom is bonded to three carbon atoms in a trigonal planar geometry. This atomic configuration produces an infinite three-dimensional covalent network with strong bonding in all directions.

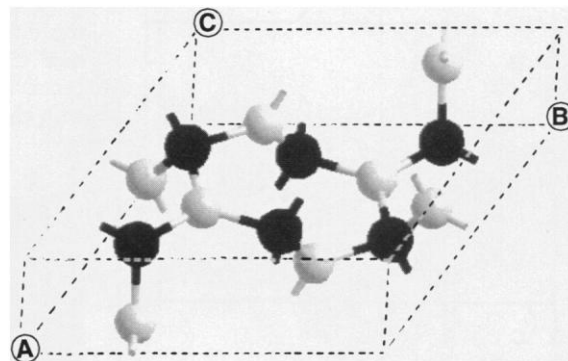
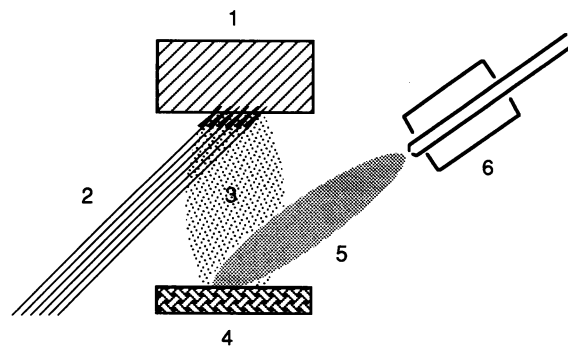


Fig. 2. Schematic diagram of the thin film growth apparatus. The graphite target (1), is continuously rotated while irradiated by the output from a frequency-doubled Nd:YAG laser (2). The resulting carbon ablation plume (3) is directed toward a substrate (4). The substrate is fixed to a heater that is capable of controlling the temperature between 25° and 900°C. An atomic nitrogen beam (5), which is produced using an RF discharge (6), intersects the ablation plume at the substrate. The components are housed within a stainless steel chamber evacuated using liquid nitrogen-trapped diffusion pumps having a total capacity of 10,000 liter s^{-1} .



growth between 165° and 600°C has little effect on the C:N ratio in the films. These data indicate that within this temperature range the reaction between laser-generated carbon and atomic nitrogen dominates the formation of the C-N materials.

We have also obtained data addressing the chemical nature of these C-N materials. X-ray photoelectron spectroscopy measurements (XPS) (Surface Science, Model 206) show that the C-1s and N-1s binding energies in the C-N films are 284.6 and 399.1 eV, respectively. The observed C-1s binding energy is comparable to that observed (284.3 eV) in diamond thin films (13). More importantly, the observed N-1s binding energy is comparable to that found in molecules with covalent C-N bonds. In contrast, the N-1s binding in boron nitride (a solid in which there is significant charge transfer from boron to nitrogen) is about 1 eV smaller

than we observe (14). The XPS data thus indicate that carbon and nitrogen form an unpolarized covalent bond in these new C-N materials, and thus our experimental results agree with earlier theoretical suggestions (4) that there is almost no charge transfer between C and N. The C-N films prepared with the atomic nitrogen source also exhibit excellent adhesion to both Si and Ni substrates, and, furthermore, scratch tests indicate that these films are qualitatively hard (15). In contrast, the C films obtained from deposition in 200 mtorr of N₂ without atomic nitrogen exhibit poor substrate adhesion and are very soft. Finally, the C-N films also exhibit good thermal stability. RBS analysis of the films after thermal treatments in flowing N₂ up to 800°C showed no observable loss of nitrogen. These characteristics (adhesion, hardness, and thermal stability) are all suggestive of extended C-N covalent bonding in the films and, furthermore, are promising when considering future applications.

The structure of these new C-N materials has been investigated with electron diffraction. Transmission electron microscopy (TEM) studies show that the films exhibit poor crystallinity; however, small crystallites with grain sizes <10 nm are observed in all of the C-N materials prepared with the atomic nitrogen source. Significantly, relatively sharp electron diffraction ring patterns are observed from the C-N samples (Fig. 4). Control experiments verify that the diffraction peaks are due only to the new C-N materials. First, x-ray fluorescence analyses carried out simultaneously with the electron diffraction measurements

demonstrate that there is no substrate (Si or Ni) contamination in material used in the diffraction studies. Secondly, it is not possible to index the experimental diffraction data to diamond or graphite structures (that is, possible impurities) or to Cu or CuO (that is, the TEM support). Lastly, we were unable to observe diffraction rings from the C films produced in 200 mtorr of N₂.

Notably, the diffraction patterns obtained from our new C-N materials can be indexed to the reflections expected for the β -C₃N₄ structure shown in Fig. 1. Six diffraction rings were reproducibly observed in these materials with d-spacings of 2.17, 2.10, 1.24, 1.18, 1.07, and 0.81 Å. The peaks can be consistently indexed as the (101), (210), (320), (002), (411), and (611) reflections, respectively, for the β -C₃N₄ structure. Furthermore, these experimental d-spacings are in excellent agreement with the values calculated using the theoretical lattice constants for the β -C₃N₄ structure: 2.20, 2.11, 1.27, 1.20, 1.09, and 0.80, respectively. Although additional diffraction studies will be needed to refine the atomic coordinates of this solid, our data nevertheless provide unambiguous evidence for the presence of the β -C₃N₄ structure in these C-N materials (16). It is also important to note that this is the only crystalline material we identify in the films regardless of their nitrogen content. This observation suggests that β -C₃N₄ may be the most stable extended C-N solid, and indicates that optimization of our synthetic conditions could lead to pure β -C₃N₄ materials (17). We believe that the present results offer exciting prospects for future studies of this material.

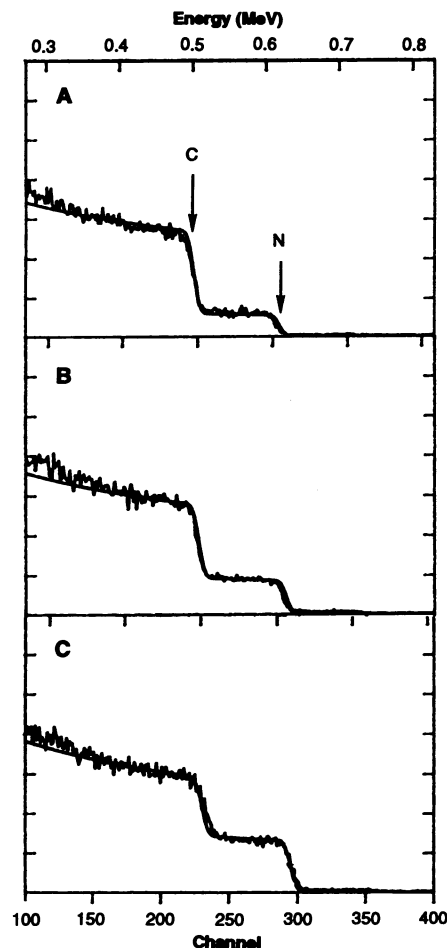


Fig. 3. RBS spectra recorded on 3- μ m-thick C-N films produced using 1% (A), 4% (B), and 12% (C) N₂ in He. The smooth solid lines through each spectra correspond to the best fit simulation from which the C-N film stoichiometries reported in the text were determined. The spectra were recorded using 2-MeV helium ions with a General Ionics Model 4117 instrument.

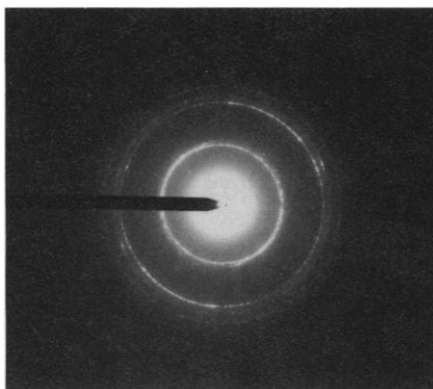


Fig. 4. Electron diffraction pattern recorded on material from a C-N film that contained 60% C and 40% N using a beam energy of 120 keV (Philips Em420T TEM). The samples were prepared for analysis by either directly scraping material onto Cu grids or grinding the C-N film, suspending the resulting particles in MeOH and then depositing the suspension onto the grid. Similar diffraction patterns were obtained using both preparative methods.

REFERENCES AND NOTES

1. R. Pool, *Science* **255**, 1077 (1992).
2. In addition, a hard material must resist fracture to be useful in many applications.
3. M. L. Cohen, *Phys. Rev. B* **32**, 7988 (1985).
4. A. Y. Liu and M. L. Cohen, *Science* **245**, 841 (1989); *Phys. Rev. B* **42**, 10727 (1990).
5. D. Hardie and K. H. Jack, *Nature* **180**, 332 (1957).
6. H.-X. Han and B. J. Feldman, *Solid State Commun.* **65**, 921 (1988).
7. L. Maya, D. R. Cole, E. W. Hagaman, *J. Am. Ceram. Soc.* **74**, 1686 (1991).
8. M. R. Wixom, *ibid.* **73**, 1973 (1990).
9. M. Y. Ming *et al.*, *Surf. Coating Technol.* **54/55**, 360 (1992).
10. A frequency-doubled Quanta Ray GCR-16 laser was used to provide 8-ns pulses of 532-nm light with an energy of 300 mJ per pulse. The roughly 10-mm-diameter Gaussian output from the laser was focused to a spot approximately 2 mm in diameter on the graphite target at a position off the rotation axis of the target.
11. H. W. Kroto, J. R. Heath, S. C. O'Brien, R. F. Curl, R. E. Smalley, *Nature* **318**, 162 (1985).
12. J. E. Pollard, *Rev. Sci. Instrum.* **63**, 1771 (1992); S. J. Sibener, R. J. Buss, C. Y. Ng, Y. T. Lee, *ibid.* **51**, (1980).
13. D. N. Belton, S. J. Harris, S. J. Schmiege, A. M. Weiner, T. A. Perry, *Appl. Phys. Lett.* **54**, 416 (1989).
14. *Handbook of X-ray Photoelectron Spectroscopy*,

- C. D. Wagner, W. M. Riggs, L. E. Davis, J. F. Moulder, G. E. Muilenberg, Eds. (Perkin-Elmer Corporation, Eden Prairie, MN, 1979), p. 40.
15. Film adhesion was measured qualitatively with an adhesive tape test. Pieces of adhesive tape were attached to the surfaces of the C-N and C films and then peeled off these surfaces. No material was removed from surfaces of the C-N films; however, significant solid was peeled from C sample surfaces. These results are indicative of good adhesion and poor adhesion, respectively. In addition, we found that dragging a hard metal needle across the surface of the C-N films does not produce observable damage, although dragging this needle across the C films produces a deep groove. Future studies of microindentation will be needed, however, to assess quantitatively the film hardness.
 16. We have further probed the structure of these films using convergent beam electron diffraction. These preliminary data, which were obtained on individual crystallites within the films, are consistent with the β - C_3N_4 structure. Single crystal materials will be needed, however, to fully resolve the structure of these C-N materials with four-circle x-ray diffraction.
 17. We believe that there are several experimental factors that may be explored in the future to increase further the average nitrogen content of

the films. First, a higher RF discharge power would increase the dissociation fraction and kinetic energy of the N atoms in the beam. Both of these effects should increase the extent of reaction with the carbon fragments and thereby increase the average N content in the films. At present, however, our atomic beam source cannot be operated at >150 W used in this study. Secondly, we believe that it will be important to control better the sizes of the carbon fragments produced by laser ablation since larger carbon fragments may not react completely with the atomic nitrogen beam. Variations in the laser power density and photofragmentation of the ablated carbon species are two strategies that we are currently using to study how the carbon fragment size affects the extent of reaction with atomic nitrogen.

18. We acknowledge J. E. Pollard for helpful discussions and D. R. Herschbach for the loan of the diffusion pumps used in these studies. C.M.L. acknowledges support of this work through a National Science Foundation–Presidential Young Investigator award and the NSF-supported Materials Research Laboratory at Harvard.

10 May 1993; accepted 4 June 1993

Interlayer Tunneling and Gap Anisotropy in High-Temperature Superconductors

Sudip Chakravarty, Asle Sudbø, Philip W. Anderson, Steven Strong

A quantitative analysis of a recent model of high-temperature superconductors based on an interlayer tunneling mechanism is presented. This model can account well for the observed magnitudes of the high transition temperatures in these materials and implies a gap that does not change sign, can be substantially anisotropic, and has the same symmetry as the crystal. The experimental consequences explored so far are consistent with the observations.

The gap in the electronic spectrum at the Fermi energy is a distinguishing feature of a superconductor; it is also the order parameter that describes the broken symmetry of the superconducting phase. The macroscopic properties of a superconductor follow once the gap is known. Here we explore a gap equation that was recently proposed by one of us (1) to explain the properties of the high-temperature cuprate superconductors. The underlying mechanism that leads to this gap equation is an interlayer tunneling phenomenon. We show (i) that the high transition temperatures of these materials can be natural consequences of this mechanism, (ii) that the superconducting gap can exhibit substantial anisotropy similar to that observed in recent photoemission measurements (2) but does not change sign (it is not possible to detect the sign of the gap in photoemission experiments), and (iii) that the superconducting state does not

exhibit a Hebel-Slichter peak in the nuclear magnetic relaxation rate. Because the gap does not change sign and has the same symmetry as the crystal, even a moderate amount of nonmagnetic impurity scattering is likely to have little effect on the superconducting transition temperature T_c . We refer to this gap as an anisotropic s -wave gap.

The interlayer tunneling mechanism (1) is based on the presence of well-defined CuO layers in these materials. The idea is to amplify the pairing mechanism within a given layer by allowing the Cooper pairs to tunnel to an adjacent layer by the Josephson mechanism. This delocalization process of the pairs gives rise to a substantial enhancement of pairing only if the coherent single particle tunneling between the layers is blocked, which we argue to be the case on phenomenological as well as theoretical grounds. In this sense the presence of bilayers or triple layers in these materials is important. The principle of amplification, however, is indifferent to the specific mechanism within a given CuO layer; the pairing can be due to electron-phonon interaction

or spin fluctuations (3). We shall assume that the electron-phonon interaction is the dominant mechanism. As shown below, this leads to a natural explanation of the anomalous isotope effect seen in these materials. It is known that the isotope effect is negligibly small for materials with the highest T_c 's and reverts to near normal for very low ones.

The normal state of these materials exhibits properties that require us to go beyond the conventional Fermi liquid theory (4). Here we assume that, owing to strong electronic correlation effects, coherent single particle tunneling is not possible between the adjacent layers of a given bilayer even though the bare hopping rate, as obtained from electronic structure calculations, is substantial, of the order of 0.1 eV—a phenomenon that has been termed confinement (1). To justify this assumption, we briefly recall the phenomenology of the normal state of the high-temperature superconductors; for a more complete discussion, see (4).

Suppose for the moment that the normal state is described by a Fermi liquid. Then, the two CuO layers hybridized by the single particle tunneling matrix element, $t_{\perp}(\mathbf{k})$, would lead to a symmetric and an antisymmetric combination of the quasiparticle states for each value of the wave vector \mathbf{k} in the plane. (Throughout this report, \mathbf{k} will refer to a two-dimensional wave vector.) Because these states are dipole-active, the transition between them should lead to a prominent signature in the frequency-dependent c -axis conductivity, which, to date, has not been observed. [Because of the \mathbf{k} dependence of $t_{\perp}(\mathbf{k})$, the signature is likely to be broad, but should still be observable in the range 500 to 1000 cm^{-1} .] In contrast, if the one-particle Green's function does not exhibit a quasiparticle pole but a power-law relaxation for asymptotically long times, the coherent quasiparticle tunneling can be blocked as a result of the orthogonality catastrophe (5). The observation of a rapidly growing c -axis resistivity with decreasing temperature in these materials (6) is also consistent with the confinement idea. Note that the observed Fermi surface in photoemission experiments does not establish the Fermi liquid behavior of the normal state; as a counter example, it is only necessary to recall the well-established Luttinger liquid behavior of one-dimensional interacting Fermi systems (7). Thus, the Fermi surface defined as the surface of low-energy excitations in \mathbf{k} -space that encloses a volume appropriate to the density of electrons can exist in a non-Fermi liquid; in this case, the singularity in the derivative of the electronic occupation number at the Fermi surface will be a power-law instead of a δ function.

S. Chakravarty and A. Sudbø, Department of Physics, University of California—Los Angeles, Los Angeles, CA 90024.

P. W. Anderson and S. Strong, Department of Physics, Princeton University, Princeton, NJ 08544.